

Design and Implementation of a Quasiholonomic Mobile Robot

Alessio Salerno

Department of Mechanical Engineering
Columbia University
220SW Mudd Mail-Code: 4703
500W 120th Street
New York, NY 10027, USA
as2948@columbia.edu

Jorge Angeles

Department of Mechanical Engineering &
Centre for Intelligent Machines
McGill University
817 Sherbrooke West
Montreal, QC, H3A 2K6 Canada
angeles@cim.mcgill.ca

Abstract—Aspects of the mechatronic design and prototyping of a robot designed and realized with the quasiholonomy property are discussed here. After an overview of the motivation and applications of the project at hand, we show how we faced the challenges encountered in the mechatronic design and implementation of the prototype. The actuation system and power supply dimensioning are then described, along with the selection of the on-board control unit and programming of the real-time operating system. Advantages of quasiholonomic robotic systems are substantiated.

I. INTRODUCTION

This paper focuses on the mechatronic aspects in the design and prototyping of a quasiholonomic (QH) mobile robot. In particular, we built a prototype of a mobile robot designed to be QH, quasiholonomy being a property that eases, in principle, the control of nonholonomic (NH) systems [1]. This property has been extensively discussed in [2] and [3]. *Quasimoro* is a QH mobile robot having two actuated coaxial conventional wheels, without any caster, and an intermediate body (IB) that carries the payload, as illustrated in Fig. 1.

The first prototype of *Quasimoro*, designed and implemented at McGill's Centre for Intelligent Machines (CIM), relies on a dead-reckoning multi-sensor system, which consists of two optical incremental encoders mounted on the motor shafts, to sense the relative angular positions and angular

velocities (by numerical differentiation) of the wheels with respect to the intermediate body. The robot is also equipped with a solid-state tilt sensor to measure the inclination and angular velocity (by numerical differentiation) of the IB with respect to the vertical. The absolute angular positions (velocities) of the wheels are readily measured as the algebraic sum of the relative wheel positions (velocities) with respect to the IB and the angular position (velocity) of the IB itself.

In [4] the authors reported aspects of modeling and controllability of quasiholonomic two-wheeled robots. The development of a control algorithm for the system at hand is studied in [5], while the mechanical conceptual design of *Quasimoro* is presented in [6]. Design conditions for quasiholonomy are given in [7], while the embodiment mechanical design is provided in [8]. This work presents the mechatronic design of the first prototype of *Quasimoro*.

II. MOTIVATION

The motivation behind the *Quasimoro* project is manifold: *i*) to validate the theoretically proven advantages introduced by quasiholonomy in the computed torque control of non-holonomic mechanical systems [4]; *ii*) to improve understanding of the effect of caster wheels on trajectory tracking of mobile robots ¹; *iii*) to determine the conditions under which dynamic, as opposed to kinematic, control of mobile robots becomes necessary; *iv*) to elucidate the advantages and disadvantages in the implementation of control strategies for mobile robots based on the inclusion of the robot dynamics; *v*) to validate control strategies which feature robustness with respect to payload variations [5]. Another significant impact of the project is on the field of robotics for human augmentation (RHA). Different from service robotics, which focuses on *general purpose machines*, RHA is a branch of robotics aiming at solving *specific problems* brought about by the impairments of the disabled user, and integrating humans and robots in the same task [9]. *Quasimoro* has been designed to operate as an assistive device for the mobility-challenged.

¹To do this the robot has been designed to allow for one or more arbitrarily located caster wheels (not essential for normal operation).

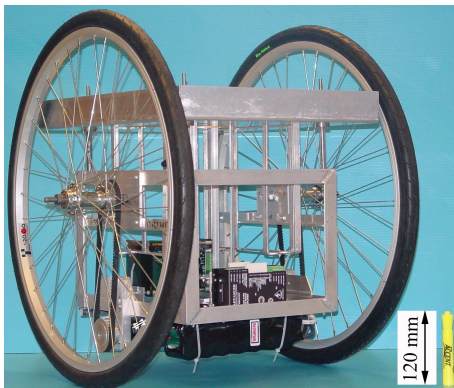


Fig. 1. *Quasimoro* prototype

For paraplegic wheelchair users, who make up most of the mobility-challenged, it is very difficult to maneuver a wheelchair while balancing a tray with food and drinks and extremely inconvenient to move around every time that they need an item, e.g. a flask of medication or a book. Quasimoro is designed to act as a *waiter* of the wheelchair user, who no longer would have to struggle to accomplish a task by moving around. The user envisioned can simply have the robot carry out her tasks by using a joypad, or pushing a button, or even issuing a voice command. More specifically, the final application of the robot will be in an environment specifically designed to study how to improve the living conditions of a wheelchair user [6]. Significant contributions to the fields of mechatronics and embedded robotic systems are expected. As a matter of fact, the Quasimoro project also contributes to validate a design methodology of mobile (legged, wheeled or hybrid) and underwater robots that has been developed during the last decade at McGill's CIM [10]–[13].

III. ADVANTAGES OF QUASIHOLONOMY

Let us consider a *catastatic*² mechanical system \mathcal{M} subject to p first-order scleronomous NH constraints with n positional degrees of freedom [2], namely,

$$\mathbf{A}(\mathbf{q})\dot{\mathbf{q}} = \mathbf{0}, \quad (1)$$

where \mathbf{A} is the $p \times n$ constraint matrix and \mathbf{q} is the n -dimensional vector of generalized coordinates. In this case the kinetic energy is a quadratic homogeneous function of the generalized velocities [2] and the constrained Lagrangian takes the form

$$\tilde{L}(\mathbf{q}, \mathbf{u}) = \frac{1}{2} \mathbf{u}^T \mathbf{I}(\mathbf{q}) \mathbf{u} - V(\mathbf{q}), \quad (2)$$

where: $\mathbf{I}(\mathbf{q}) = \mathbf{N}^T \mathbf{M} \mathbf{N} > 0$; $\mathbf{M}(\mathbf{q})$ is the *unconstrained generalized inertia matrix*; \mathbf{N} is an orthogonal complement of the constraint matrix \mathbf{A} , of $m(=n-p) \times n$; \mathbf{u} is the m -dimensional vector of independent generalized-velocities; and $V(\mathbf{q})$ is the potential energy. Moreover, the unconstrained generalized momentum takes the form

$$\mathbf{p} = \frac{\partial L(\mathbf{q}, \dot{\mathbf{q}})}{\partial \dot{\mathbf{q}}} = \frac{\partial}{\partial \dot{\mathbf{q}}} \left(\frac{1}{2} \dot{\mathbf{q}}^T \mathbf{M} \dot{\mathbf{q}} - V \right) = \mathbf{M} \dot{\mathbf{q}} = \mathbf{M} \mathbf{N} \mathbf{u}, \quad (3)$$

The *holonomy matrix* of the system was defined in [7] as

$$\mathbf{H} = \frac{\partial \mathbf{N} \mathbf{u}}{\partial \mathbf{q}} \mathbf{N} - \dot{\mathbf{N}}.$$

Definition 3.1: A system is *quasiholonomic* iff $\mathbf{H} \neq \mathbf{O}_{n \times m}$ and $\mathbf{H}^T \mathbf{p} = \mathbf{0}_m$.

Quasiholonomy brings about several advantages in the control of NH mechanical systems. As proven in the sequel, quasiholonomy simplifies the computed-torque control (CTC) of NH systems. Therefore, the partial linearization of NH systems [14]–[16], is simplified as well.

²In the realm of classical mechanics, a system is called “catastatic” when, upon setting all its generalized velocities to zero, its kinetic energy vanishes; otherwise, the system is termed *acatastatic*.

Assuming that the number of external inputs equals the mobility m of the system, its mathematical model is

$$\dot{\mathbf{I}} \mathbf{u} + \mathbf{n}(\mathbf{q}, \mathbf{u}) = \mathbf{N}^T \mathbf{S} \boldsymbol{\tau}, \quad (4)$$

where \mathbf{S} is a full-rank $n \times m$ matrix mapping the m -dimensional vector of external inputs [16] $\boldsymbol{\tau}$ into the vector of unconstrained generalized forces and

$$\mathbf{n}(\mathbf{q}, \mathbf{u}) = \dot{\mathbf{I}} \mathbf{u} - \frac{\mathbf{N}^T}{2} \left(\frac{\partial}{\partial \mathbf{q}} (\mathbf{u}^T \mathbf{I} \mathbf{u}) \right) + \mathbf{N}^T \frac{\partial V}{\partial \mathbf{q}} + \mathbf{H}^T \mathbf{M} \mathbf{N} \mathbf{u}. \quad (5)$$

The $(n+m)$ -dimensional *reduced state-space model*, obtained by merging the kinematic model of eq. (1) and the dynamics model of eq. (4) is given by [16]

$$\begin{aligned} \dot{\mathbf{q}} &= \mathbf{N}(\mathbf{q}) \mathbf{u}, \\ \dot{\mathbf{u}} &= \mathbf{I}^{-1}(\mathbf{q}) \mathbf{N}^T(\mathbf{q}) \mathbf{S}(\mathbf{q}) \boldsymbol{\tau} - \mathbf{I}^{-1}(\mathbf{q}) \mathbf{n}(\mathbf{q}, \mathbf{u}). \end{aligned}$$

Introducing the non-restrictive assumption that the $m \times m$ matrix $\mathbf{N}^T \mathbf{S}$ is non-singular [17], we perform a partial linearization of the reduced state-space model via a CTC scheme, thereby obtaining

$$\boldsymbol{\tau} = [(\mathbf{N}^T(\mathbf{q}) \mathbf{S}(\mathbf{q}))^{-1} (\mathbf{I}(\mathbf{q}) \mathbf{a} + \mathbf{n}(\mathbf{q}, \mathbf{u}))] \quad (6)$$

where $\mathbf{a} \in \mathbb{R}^m$ is a new vector of control inputs, which is obtained by the application of linear control strategies. The system thus resulting is

$$\begin{aligned} \dot{\mathbf{q}} &= \mathbf{N}(\mathbf{q}) \mathbf{u}, \\ \dot{\mathbf{u}} &= \mathbf{a}, \end{aligned}$$

where the first equation represents the n -dimensional kinematic model and the second equation acts as a m -dimensional dynamic extension [16]. Vector \mathbf{a} can be chosen as $\mathbf{a} = -\mathbf{K}_p \mathbf{q} - \mathbf{K}_d \dot{\mathbf{q}} + \mathbf{r}$, where $\mathbf{r} = \ddot{\mathbf{q}}_d + \mathbf{K}_d \dot{\mathbf{q}}_d + \mathbf{K}_p \mathbf{q}_d$, \mathbf{q}_d is the vector of desired generalized coordinates, \mathbf{K}_d and \mathbf{K}_p being two positive definite gain matrices [18].

Hence, it is possible to cancel dynamic terms via non-linear feedback assuming that the dynamics model is exactly known, and that the complete system state is measurable [16]. Hence, from definition 3.1, we have,

Claim 3.1: If \mathcal{M} is quasiholonomic, the last term $\mathbf{H}^T \mathbf{M} \mathbf{N} \mathbf{u}$ of eq. (5) vanishes, thereby reducing the computational complexity of the computed-torque controller described in eq. (6).

Remark 3.1: If, besides being QH, \mathcal{M} is *underactuated*, i.e. $\boldsymbol{\tau}$ is l -dimensional, with $l < m$, then Claim 3.1 still holds.

This remark can be readily proven by noting that if \mathcal{M} is QH and underactuated, then one can still conduct a *partial linearization* [19] of eq. (4). This can be done via a CTC scheme, in order to linearize the l equations of eq. (4), in which $\boldsymbol{\tau}$ explicitly appears. If \mathcal{M} is QH, the foregoing scheme will simplify in the same way as eq. (6) did, since $\mathbf{H}^T \mathbf{M} \mathbf{N} \mathbf{u}$ vanishes.

Implementation of CTC schemes requires the right-hand side of eq. (6) to be computed in real time. This computation is to be performed at sampling times of the order of 1 ms so as to comply with Shannon's Theorem [20] and ensure that the assumption of operating in the continuous time

domain is realistic [18]. This may pose severe constraints on the hardware/software architecture of the robot control system [18]. To cope with this issue, one can lighten the computations involved in eq. (6) by *designing* the system with quasiholonomy. It is noteworthy that the computational complexity is strongly reduced in the case of large-scale systems. Moreover, one can readily infer that for a QH system: *i*) the implementation of the control scheme (6) will return a faster controller, since, in principle, fewer floating-point operations (flops) per second will be required for the computation of the command signal; *ii*) the computational complexity of CTC algorithms will be reduced; *iii*) the implementation of the control scheme (6) will return a more accurate controller, since the round-off error will be smaller, the computation of the command signal requiring fewer numerical calculations; and *iv*) if \mathbf{u} is a total time-derivative, standard control strategies for holonomic systems, such as robotic manipulators [18], can be applied to control the virtual holonomic system³. In this light, QH systems turn out to be extremely useful when the dynamics model is needed in their control, for example, in applications imposing high speeds, high loads, or both [21], [22].

For a generic wheeled mobile robot (WMR) composed of a main body and N conventional, off-centered orientable wheels with independently powered steering and rotation axes, $\mathbf{H}^T \mathbf{M} \mathbf{N} \mathbf{u}$ takes the form [7]

$$\mathbf{H}^T \mathbf{M} \mathbf{N} \mathbf{u} = \frac{1}{l^3} \left(\frac{mr^2}{4} + J_b \right) \sum_{i=1}^N \begin{bmatrix} \mathbf{E}^T \dot{\mathbf{p}}_i \\ -b \dot{\mathbf{c}}^T \mathbf{e}_i \end{bmatrix} \eta_i^T \dot{\mathbf{p}}_i \quad (7)$$

in which b is the distance between the center of the robot platform C and the wheel steering axis; \mathbf{c} is the position vector of C in the inertial frame; \mathbf{e}_i is the unit horizontal vector directed from the steering axis of the i th wheel to C ; $\mathbf{p}_i = \mathbf{c} + b \mathbf{e}_i$; \mathbf{E} is a 2×2 matrix rotating vectors through 90° CCW; and η_i is the horizontal unit vector directed from the axis of rotation of the i th wheel to C .

The number of flops associated with the computation of the coefficient of the foregoing summation is $9M + 1A$, where M indicates a multiplication, A an addition. Moreover, for each of the terms of the foregoing sum we record the number of flops in Table I. Moreover, performing the sum

\mathbf{p}_i	\leftarrow	$\mathbf{c}_i - l \xi_i$	$(2M + 2A)$
$\dot{\mathbf{p}}_i$	\leftarrow	$\dot{\mathbf{c}}_i - l(\dot{\psi} + \dot{\psi}_i) \eta_i$	$(4M + 4A)$
$\eta_i^T \dot{\mathbf{p}}_i$			$(2M + 1A)$
$-b \dot{\mathbf{c}}^T \mathbf{e}_i$			$(4M + 1A)$
$\mathbf{E}^T \dot{\mathbf{p}}_i$			$(4M + 2A)$
$\begin{bmatrix} \mathbf{E}^T \dot{\mathbf{p}}_i \\ -b \dot{\mathbf{c}}^T \mathbf{e}_i \end{bmatrix} \eta_i^T \dot{\mathbf{p}}_i$			$3M$
			$(19M + 10A)$

TABLE I
NUMBER OF FLOPS

of eq. (7) entails $3(N - 1)A$. Therefore, the number N_f of flops associated with the computation of $\mathbf{H}^T \mathbf{M} \mathbf{N} \mathbf{u}$ reduces to $N_f = (19N + 9)M + (13N - 2)A$. Hence, the amount of flops

³In this case, i.e., with \mathbf{u} a total time-derivative, \mathcal{M} becomes a Chaplygin system.

saved by virtue of quasiholonomy for this type of robots is N_f .

The quasiholonomy property introduces also a few advantages for the numerical analysis of NH systems. Since the nonholonomy term vanishes, the integration of the Lagrange equations is correspondingly faster (fewer flops) and more accurate (reduced round-off error) [7].

The main simplification introduced by quasiholonomy in the analysis and control of nonholonomic systems lies in that their dynamics model can be represented using the typical form of Lagrange's equations that is valid for holonomic systems.

IV. MECHANICAL DESIGN

A. Design for Quasiholonomy

Let Π_m be the plane equidistant from the midplanes of the two wheels. Quasiholonomy requires that robot mass center lie in Π_m .

In order to locate the mass center of the robot on Π_m , symmetry with respect to this plane was respected throughout the design process. Moreover, for stability, all the robot components, such as motors, power supply, electronic equipment, were placed as low as possible. Finally a control algorithm which features robustness with respect to payload-variations was derived in [5] in order to stabilize the IB throughout the robot motion.

B. Embodiment Design

The mechanical design guidelines and specifications were mainly dictated by the constraints present in the environment where the robot operates, i.e. living quarters specifically designed for wheelchair users, and the limitations on the mobility of the user. Therefore, issues, such as doorway negotiation, access to the payload by the user and ground clearance dictated the dimensions of the robot chassis [6].

Exploiting the techniques of virtual prototyping, several design solutions were derived in a CAE environment [8]. The first virtual prototype, depicted in Fig. 2a, consisted of *i*) two custom-made wheels supplied with elastomeric O-ring belts that acted as tires, *ii*) a custom-fabricated cage made of four aluminum alloy braces for guaranteeing the parallelism between the wheels, and *iii*) a bolted chassis.

Challenges such as the effect of rolling friction and wheel axis alignment on the positioning accuracy of the robot were faced and successfully overcome at this stage. In order to lower the overall mass centre of the robot, to limit the width of the robot and to contain the bending moment of

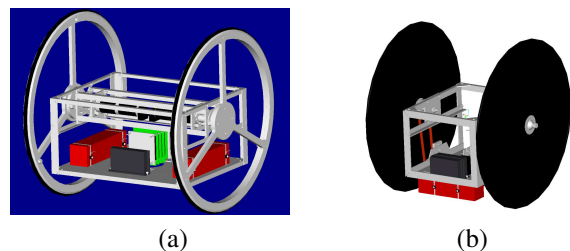


Fig. 2. Virtual prototyping: (a) first concept; (b) final concept.

the planetary gearhead output shaft, the rigid transmission between planetary gearhead output shaft and the wheel was replaced with a timing-belt transmission. With the intention of reducing manufacturing costs, commercial front bicycle wheels were chosen, as opposed to their custom-made counterparts. The motion transmission between motor and wheel was accomplished by a couple of *Shaftloc*TM shaft-couplers by *SDP-SI* interposed between the bicycle wheel—free from bearings, spacers, nuts and axle—and a custom-made shaft (driven by the timing-belt transmission) that turns with respect to the robot chassis by means of a roller bearing. Although this solution allows for sensor redundancy and for direct sensing of the wheel rotation (e.g. by means of an optical encoder that might be housed in the robot chassis and connected to the custom-made shaft), we discarded it. There were several reasons behind this decision, which was mainly dictated by the need for simplicity and cost reduction, along with the possibility of investigating the effect of toe and camber angle variation on relatively low-speed vehicles. To do this, the front bicycle wheels and custom-made shafts were replaced, along with their bearings, with rear bicycle wheels. In order to transmit torque to the wheels, a timing pulley was threaded, screwed and glued on the traditional threaded hub—minus the freewheel mechanism [23] and the sprocket(s)—of a rear bicycle wheel, as depicted in Fig. 3. Moreover, most of the beams composing the robot chassis were welded together, thus saving time and money on robot maintenance by reducing to a minimum the number of screws that need to be periodically retightened. Furthermore, with this final design solution, depicted in Fig. 2b, we have the possibility of modifying the wheel camber, and the toe angle by simply interposing wedges between the wheel plate, on which the bicycle wheel shaft is fastened, and the robot chassis, as per Fig. 3.

The core of the mechanical structure was conceived, designed and fabricated so as to be easily interfaced to different devices that would be custom-made for complying with different applications in other fields, such as entertainment, surveillance and medical robotics (as an assistive device for hospital patients) rather than robotics for human augmentation. However, for the specific application of robotics assisting of wheelchair users, a specialized payload-holder module was designed to be easily removed from the robot and to hold books, medications, food, drinks and any other



Fig. 3. Driven pulley—close-up

item that the user might need on a daily basis, as depicted in Fig. 4. Under full payload, i.e. 75N, the robot preserves its stability at rest without any need of powering the motors, as opposed to SegwayTM [24], [25] and other self-balancing two-wheeled systems [4].

V. ELECTRICAL AND ELECTRONIC DESIGN

In the framework of modern mechatronics, the electrical and electronics aspects in the design and implementation of Quasimoro were not decoupled from the mechanical ones outlined in the previous section. As a matter of fact, in selecting the type of controller, we had to devise a system that: *i*) would be limited in dimension in order to easily fit inside the robot chassis, *ii*) would be lightweight in order to make the robot easily transportable, and *iii*) would have sufficient processor speed, memory size and I/O precision in order to implement dynamics model-based control strategies.

The on-board control unit of modern mobile robots relies mainly on the knowledge of the kinematics of the system at hand. Therefore, most of the time a micro-controller would do the job, the computational cost of kinematic control algorithms being not significant for such devices. However, if the objective is to implement model-based control strategies, such as computed torque, we need to select controllers with higher performance than micro-controllers. In this light we selected a PC/104 computer board for the Quasimoro controller. This reason is twofold: fast prototyping (PC/104 know-how being readily available at McGill's CIM) and the validation of a robot design methodology developed at McGill's CIM [10]–[13].

The layout of the electronic equipment was designed in such a way that it could be easily serviced, much like a drawer, as shown in Fig. 5. The base plate of the robot, made of AL6061T6, was designed for hosting the PC/104 stack, power amplifiers and battery packs; the latter are located below the platform in order to lower the robot mass center in a balanced (front-back) way. Therefore, the base plate is practically parallel to the ground when the system is unloaded and at rest.

A. Actuation System and Power Supply Dimensioning

The Quasimoro actuation system consists of two identical units, shown in Fig. 6, consisting of: *i*) a Maxon RE 40

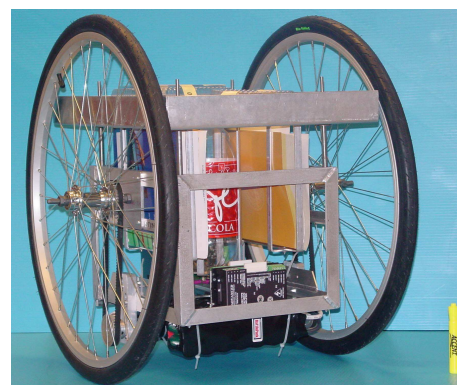


Fig. 4. Quasimoro—under full payload

(148867) brushed precision motor, equipped with a planetary gearhead (PG), namely, a Maxon GP 42 C (203123); and *ii*) a digital encoder HP HEDS N5540 A11 [26]. The PG is secured to the motor mount by means of four screws. The motor mount has three vertical slots in which three nut-bolt sets that secure the motor mount to the robot chassis are located; the foregoing slots are designed for belt tension regulation. A timing belt pulley is secured to the PG output shaft by means of a key and two set screws.

In order to guarantee the wheel rolling under any payload condition, the torque applied to the wheel cannot be higher than 10Nm, value obtained considering the sliding friction coefficient of rubber on rubber [27] and using a safety factor of 1.25. Moreover, in order to dimension the actuation system we conducted a series of numerical simulations in Matlab 6.5.1.199709 and Simulink 5.1 (R13SP1) using the variable-step solver ODE45 (Dormand-Prince). In order to set-up the simulations we assumed: *i*) that the robot undergoes motion on a planar surface; *ii*) that the robot wheels are always in contact with the ground; and *iii*) linear viscous damping in the bearings, which was accounted for by means of a Rayleigh dissipation function [28]. The viscous damping coefficient b was estimated by simulating the open-loop dynamics of the system under a rectilinear motion with an initial velocity of 2m/s. We assumed an exponential decay of the robot velocity to 0.2m/s in time T under the effect of gravity and damping. To be on the safe side two different values of T were used: $T = 10$ s and $T = 50$ s, which returns $b = 0.275$ Nms/rad and $b = 0.000275$ Nms/rad, respectively. The PRO/Engineer-calculated values of the geometric and inertial parameters of the robot, for a minimum payload (i.e. no payload) and a maximum payload are displayed in Table II. m_3 indicates the mass of the IB, m the mass of a single wheel, r the wheel radius, l the wheel-center distance, d the distance of the robot mass center C_3 from the midpoint C of the segment linking the wheel centers, J_1 the moment of inertia of the robot about the axis passing through C and C_3 , while J_2 is the moment of the inertia of the robot about the wheel axis.

The robot direct dynamics and kinematics were simulated

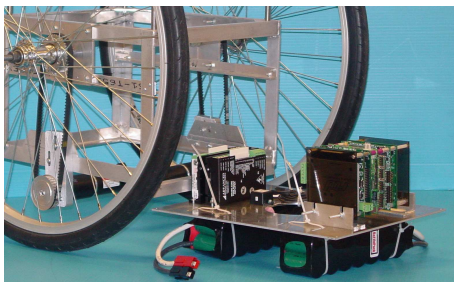


Fig. 5. Electronic equipment servicing

Payload	J_1, J_2 [kg m ²]	m, m_3 [kg]	d, r, l [m]
Minimum	0.402, 0.588	2.507, 15.275	0.113, 0.305, 0.448
Maximum	0.531, 0.851	2.507, 22.735	0.061, 0.305, 0.448

TABLE II

GEOMETRIC AND INERTIAL PARAMETERS

along with a multi-variable state-feedback controller [5]. As shown in [8] the most exciting maneuver is the one in which the robot climbs a 20%-slope following a rectilinear path under full payload, starting with the IB rotated 90° with respect to the vertical in the direction of motion. While also taking into account the moments of inertia of the driving pulleys, motor rotors and PG, several simulations were conducted, which, for brevity, are not reported here. In order to be on the safe side, two different sets of simulations were run: one adopting the PRO/Engineer-calculated geometric and inertial parameters of the robot, the other adopting as geometric and inertial parameters of the robot the preceding parameter values multiplied by a safety factor of 1.5. Each of the preceding simulation sets were themselves split into subsets, namely, one using $b = 0.275$ Nms/rad, the other using $b = 0.000275$ Nms/rad. Applying the PG-motor selection procedure [26] for each of the simulations, the above motor/gearhead combination was repeatedly obtained. The selection of the motor manufacturer was governed by the wide availability of gearhead and motor pairs, good specific power (power output/mass) and low rotor inertia.

Knowing the torque constant of the selected motor, $K_t = 0.030$ Nm/A [26], the desired maximum continuous current and the desired peak current are $i_{cont} = \tau_{rms,m}/K_t = 5.011$ A and $i_{peak} = \tau_{max,m}/K_t = 6.285$ A, respectively. These parameters led to the selection of the Advanced Motion Control 25A8 amplifiers, shown in Fig. 7, which can safely source up to twice the required continuous current, with an internal limit set prior to installation.

In motion control applications, two important factors have to be taken into account when dimensioning the power supply: the internal resistance and the nominal voltage. Quasimoro is powered by four Nickel-metal Hydride battery packs arranged in series, each pack having seven *Sanyo Twicell HR-D* cells. This set-up is characterized by $V_{nom} = 33.6$ V and $R_{in} = 0.084\Omega$ [29], which is low enough not to hamper the robot controller performance [5]. Moreover, the nominal voltage was selected as 1.4 times the nominal voltage of the motor for a better exploitation of the actuator [8]. The battery packs feature an overall minimum autonomy of 10 hours.

B. On-Board Control Unit

The *Cool RoadRunner II* was selected as the PC/104 computer board [30], shown in Fig. 7. This all-in-one board

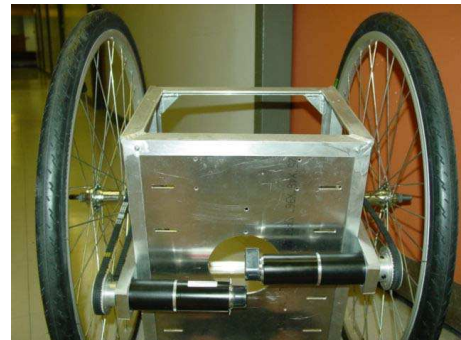


Fig. 6. Actuation system

by Lippert features a 300MHz Pentium® Class CPU, which is fast enough for implementing model-based control strategies [31]. Moreover, it does not require active cooling and has all the peripherals that constitute a PC on board along with 256 Mbyte SDRAM and CompactFlash™ socket. In order to implement real-time control algorithms a dedicated operating system (OS) was selected. The QNX 6.1 OS was installed on a 256 MByte compact flash card by Kingston. In order to execute the installation of QNX, a keyboard, monitor, mouse (serial), ethernet and CD/DVD-ROM were required. Connecting the ethernet line to a desktop or laptop computer is the first mode of communication with the robot; this mode was mainly used for configuring the OS on the on-board computer, while data logging/acquisition will happen by means of two modes of wireless communication, as described below.

C. Communication

In order to supply the robot with wireless communication capabilities, a PC/104 PCMCIA module, namely, the PCM-3115 by Versallogic [32], was stacked on to the Lippert board, shown in Fig. 7. An Orinoco Classic Gold wireless card was used in conjunction with the PCM-3115 to provide two modes of communication:

- *access-point*: the communication link between the robot and a desktop computer will be established indirectly by means of a wireless network access-point, or
- *peer-to-peer*: the communication link between the robot and a laptop computer will be established directly by their two network cards.

VI. SUMMARY

A proof that quasiholonomy simplifies the computed-torque control of nonholonomic systems is provided. Crucial aspects of the mechatronics design and implementation of the first prototype of a quasiholonomic mobile robot were reported here. After having given the motivation behind the research, the mechanical design and its challenges were outlined. Electrical and electronics design and implementation issues were discussed to shed light on the intricacies of the system integration of modern embedded systems. In particular, a set of different communication links between robot and user was also given. This work can be seen as a template of a design methodology developed at McGill's

CIM in the prototyping of mobile (ground or underwater) robots [10]–[13].

VII. ACKNOWLEDGMENTS

This work was completed while Alessio Salerno was with the Centre for Intelligent Machines, McGill University. This work was made possible by NSERC, Canada's Natural Sciences and Engineering Research Council, under Research Grant A4532 and by FQRNT, *Le Fonds Québécois de la Recherche sur la Nature et les Technologies*, under Equipment Grant F11500-G204754. The two-year "Hydro-Québec" McGill Major Fellowship granted to Alessio Salerno is highly acknowledged.

REFERENCES

- [1] A. Salerno, *Design, Dynamics and Control of a Fast Two-Wheeled Quasiholonomic Robot*. Montreal: Ph.D. Thesis, McGill University, 2006.
- [2] S. Ostrovskaya and J. Angeles, "Nonholonomic systems revisited within the framework of analytical mechanics," *Applied Mechanics Reviews*, vol. 51, no. 7, pp. 415–433, 1998.
- [3] S. Ostrovskaya, *Dynamics of Quasiholonomic and Nonholonomic Reconfigurable Rolling Robots*. Montreal: Ph.D. Thesis, McGill University, 2001, [Online]. Available at: <http://www.cim.mcgill.ca/rmsl/Angeles.html/publications/ostrovskaya.pdf>.
- [4] A. Salerno and J. Angeles, "A new family of two-wheeled mobile robots: Modeling and controllability," *IEEE Trans. Robot.*, 2006, in press.
- [5] —, "The control of semi-autonomous two-wheeled robots undergoing large payload-variations," in *Proc. IEEE Int. Conf. Robot. Automat.*, New Orleans, 2004.
- [6] —, "The preliminary design of a novel robot for human augmentation," in *Proc. CCToMM Symposium on Mechanisms, Machines, and Mechatronics*, Montreal, Canada, May 2003.
- [7] A. Salerno, S. Ostrovskaya, and J. Angeles, "The development of quasiholonomic wheeled robots," in *Proc. IEEE Int. Conf. Robot. Automat.*, Washington D.C., 2002.
- [8] A. Salerno, R. Perlin, and J. Angeles, "The embodiment design of a two-wheeled self-balancing robot," in *Proc. The Inaugural CDEN Conference*, Montreal, Canada, July 2004.
- [9] G. Bolmsjö, H. Neveryd, and H. Eftving, "Robotics in rehabilitation," *Trans. Rehabilitation Engineering*, vol. 3, no. 1, pp. 77–83, March 1995.
- [10] U. Saranlı, M. Buehler, and D. E. Koditschek, "Rhex — a simple and high mobile hexapod robot," *International Journal of Robotics Research*, vol. 20, no. 7, pp. 616–631, July 2001.
- [11] C. Steeves, M. Buehler, and S. G. Penzes, "Dynamic behaviors for a hybrid leg-wheel mobile platform," in *Proc. SPIE 2002*, vol. 4715, Orlando, FL, 2002, pp. 75–86.
- [12] J. A. Smith and I. Poulakakis, "Rotary gallop in the untethered quadrupedal robot Scout II," in *IEEE/RSJ Int. Conf. Intell. Robots and Syst.*, Sendai, Japan, 2004.
- [13] C. Prahacs, A. Saunders, M. K. Smith, D. McMordie, and M. Buehler, "Towards legged amphibious mobile robotics," in *Proc. The Inaugural CDEN Conference*, Montreal, Canada, July 2004.
- [14] B. d'Andrea-Novell, G. Bastin, and G. Campion, "Dynamic feedback linearization of nonholonomic wheeled mobile robots," in *Proc. IEEE Int. Conf. Robot. Automat.*, Nice, France, 1992.
- [15] A. M. Bloch, M. Reyhanoglu, and N. H. McClamroch, "Control and stabilization of nonholonomic dynamic systems," *IEEE Trans. Automat. Contr.*, vol. 37, no. 11, pp. 1746–1757, 1992.
- [16] A. De Luca and G. Oriolo, "Modelling and control of nonholonomic mechanical systems," in *Kinematics and Dynamics of Multibody Systems*. J. Angeles and A. Kecskemethy, (Eds.), Springer-Verlag, Vienna, 1995.
- [17] G. Campion, G. Bastin, and B. d'Andrea-Novell, "Modelling and state feedback control of nonholonomic mechanical systems," in *Proc. IEEE 30th Conf. Decision Contr.*, Brighton, England, 1991.
- [18] L. Sciavicco and B. Siciliano, *Modelling and control of robot manipulators*. Springer, 2000.

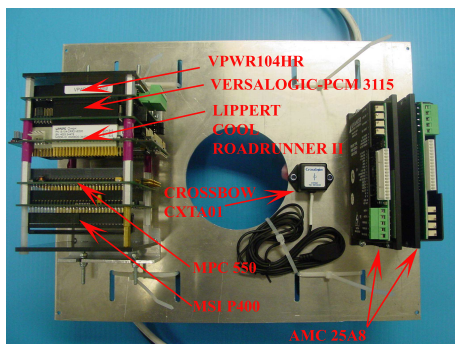


Fig. 7. On-board electronic equipment—top view

- [19] A. De Luca and G. Oriolo, "Motion planning and trajectory control of an underactuated three-link robot via dynamic feedback linearization," in *Proc. IEEE Int. Conf. Robot. Automat.*, San Francisco, CA, 2000, pp. 2789–2795.
- [20] K. J. Åstrom and B. Wittenmark, *Computer-Controlled Systems : Theory and Design*. Upper Saddle River, NJ: Prentice Hall, 1997.
- [21] S. Shekhar, "Wheel rolling constraints and slip in mobile robots," in *Proc. IEEE Int. Conf. Robot. Automat.*, New Mexico, Albuquerque, 1997, pp. 2601–2607.
- [22] D. Hong, S. A. Velinski, and X. Feng, "Verification of a wheeled mobile robot dynamic model and control ratifications," *ASME J. Dynamic Systems, Measurement, and Control*, vol. 121, no. 1, pp. 58–63, 1999.
- [23] S. Brown, "Traditional thread-on freewheels," 2003.
- [24] Segway LLC, *Segway™ Human Transporter Data-Sheet*. [Online]. Available at: <http://www.segway.com/>
- [25] D. J. Kamen, R. R. Ambrogio, R. J. Duggan, D. J. Field, R. K. Heinzmann, B. Amsbury, and C. C. Langenfeld, "Personal mobility vehicles and methods," PCT/US00/15144, Patent, Oct. 26, 2000.
- [26] Maxon Precision Motors, Inc., *Maxon Precision Motors*, 2003, catalog.
- [27] H. Frederikse and D. Lide, Eds., *CRC Handbook of Chemistry and Physics*, 76th ed. Cleveland: CRC Press, 1996.
- [28] J. Angeles, *Fundamentals of Robotic Mechanical Systems*, 2nd ed., ser. Mechanical Engineering. Springer-Verlag, New York, 2002.
- [29] Sanyo Group, *HR-D7500 Twicell Sanyo Nichel-Metal Hydride Battery Datasheet*, Mississauga, Canada, 2004, (Distributor in Eastern Canada: NICA-Power Battery Corp.).
- [30] *Cool RoadRunner II "All-in-one" PC/104-Plus CPU board — Technical Manual*, Lippert Automationstechnik GmbH, January 2001, Version 1.6. [Online]. Available at: <http://dnr.cbi.tamucc.edu/dnrpub/2003/cube/doc/TME-104P-CRR2-R1V6.pdf>
- [31] L. Villani, C. Natale, B. Siciliano, and C. Canudas de Wit, "An experimental study of adaptive force/position control algorithms for an industrial robot," *IEEE Trans. Contr. Syst. Technol.*, vol. 8, no. 5, pp. 777–786, September 2000.
- [32] *PCM-3115 User's Manual*, 3rd ed., Embedded-PC — PC/104 Modules, 1997. [Online]. Available at: <http://www.versalogic.com/Products/Manuals/m-3115b.pdf>